

# The investigation into the adsorption removal of ammonium by natural and modified zeolites: kinetics, isotherms, and thermodynamics

Min Pan<sup>1</sup>, Mingchuan Zhang<sup>2</sup>, Xuehua Zou<sup>3</sup>, Xuetong Zhao<sup>1</sup>, Tianran Deng<sup>1</sup>, Tong Chen<sup>1</sup> and Xiaoming Huang<sup>1,3\*</sup>

<sup>1</sup>Key Laboratory of Environmental Biotechnology (XMUT), Fujian Province University, School of Environmental Science and Engineering, Xiamen University of Technology, Xiamen, 361024, China

<sup>2</sup>College of Resources and Civil Engineering, Northeastern University, Shenyang, 110819, China

<sup>3</sup>Laboratory of Nanomineralogy and Environmental Material, School of Resources and Environmental Engineering, Hefei University of Technology, Hefei, 230009, China

## ABSTRACT

The objectives of this study were to modify Chinese natural zeolite by NaCl and to investigate its suitability as a low-cost clay adsorbent to remove ammonium from aqueous solution. The effect of pH on ammonium removal was investigated by batch experiments. The findings indicated that pH has a significant effect on the removal of ammonium by M-Zeo and maximum adsorption occurred at pH 8. Ion exchange dominated the ammonium adsorption process at neutral pH, with the order of exchange selectivity being  $\text{Na}^+ > \text{Ca}^{2+} > \text{K}^+ > \text{Mg}^{2+}$ . The Freundlich model provided a better description of the adsorption process than the Langmuir model. The maximum ammonium adsorption capacity was 17.83 mg/g for M-Zeo at 293K. Considering the adsorption isotherms and thermodynamic studies, the adsorption of ammonium by M-Zeo was endothermic and spontaneous chemisorption. Kinetic studies indicated that the adsorption of ammonium onto M-Zeo is well fitted by the pseudo-second-order kinetic model.  $E_a$  in the Arrhenius equation suggested the adsorption of ammonium on M-Zeo was a fast and diffusion-controlled process. The regeneration rate was 90.61% after 5 cycles. The removal of ammonium from real wastewater was carried out, and the removal efficiency was up to 99.13%. Thus, due to its cost-effectiveness and high adsorption capacity, M-Zeo has potential for use in ammonium removal from aqueous solutions.

**Keywords:** zeolite, sodium chloride modified, adsorbent, regeneration, wastewater

## INTRODUCTION

Nitrogen compounds are nutrients and are essential to all forms of life. In surface water, concentrations of ammonium nitrogen ( $\text{NH}_4^+-\text{N}$ ) exceeding 0.3–0.5 mg/L (eutrophication) can promote the growth of algae and decrease the dissolved oxygen required for aquatic life (Hussain et al., 2007). With increased awareness and understanding of the deleterious effects of nitrogen, authorities have introduced stringent laws to restrict nitrogen discharges from both wastewater treatment facilities and other point-source contributors (Karapinar, 2009). Thus, efficient removal of ammonium has gained greater attention in water and wastewater treatment.

Traditionally, ammonium removal is achieved by a typical biological nitrogen removal (BNR) process, where  $\text{NH}_4^+$  is transformed to nitrite/nitrate in the nitrification process, and then nitrite/nitrate is finally transformed to nitrogen gas through the denitrification process (Pan et al., 2015; Pan et al., 2017). However, biological systems confront great challenges in full-scale treatment plants and water bodies with low ammonium concentrations (< 5 mg/L). As an alternative to biological treatment,  $\text{NH}_4^+$  removal by ion exchange and adsorption is of great importance for nutrient removal/recycling operations (Karapinar, 2009).

Considering the benefits of low-cost and high-safety ion exchange, zeolite has been shown to be an abundant cation exchange material and is economically used in water and wastewater treatment (Widiastuti et al., 2011; Kolakovic et al., 2014; Onyango et al., 2011). Zeolites are hydrated aluminosilicates with symmetrically stacked alumina- and

silica-tetrahedrals, which results in an open and stable three-dimensional honeycomb structure possessing high cation exchange capacity, cation selectivity, higher void volume and great affinity for  $\text{NH}_4^+$  (Huang et al., 2010). However, the  $\text{NH}_4^+$  removal capacity of natural zeolite varies with the source of the zeolite, and the location within a particular deposit (Daramola et al., 2012; Zhao et al., 2010).

Malekian et al. (2011) reported the maximum  $\text{NH}_4^+$  exchange capacity of natural Iranian zeolite to be 11.31 mg/g. Sarioglu (2005) found the maximum  $\text{NH}_4^+$  exchange capacity of natural Turkish zeolite to be 25.93 mg/g. It seems that natural zeolite from different origins show different characteristics (Sarioglu, 2005). Therefore, each specific zeolite is required to be studied individually (Alshameri et al., 2014).

Additionally, the ion exchange selectivity of zeolite was reported to follow  $\text{Cs}^+ > \text{Rb}^+ > \text{K}^+ > \text{NH}_4^+ > \text{Ba}^{2+} > \text{Sr}^{2+} > \text{Na}^+ > \text{Ca}^{2+} > \text{Fe}^{3+} > \text{Al}^{3+} > \text{Mg}^{2+} > \text{Li}^+$  (Lin et al., 2013). Natural zeolite generally has a high Si/Al ratio and contains quite a few impurities, which greatly reduce its cation exchange capacity (Wang, Lin, and Pang, 2008). In order to enhance the  $\text{NH}_4^+$  adsorption capacity of zeolite, several modification methods have been applied, including microwave pre-treatment, NaOH, HCl, and NaCl solution treatment, magnetic material application, silicate-carbon solution treatment, among others (Lei, Li, and Zhang, 2008; Li et al., 2011; Liu et al., 2013). Many studies have proved that natural zeolite treated by NaOH solution could transform low-grade natural materials to high capacity cation exchangers (Wang, Lin, and Pang, 2008). However, in many of those studies, the long time of conversion, high temperature, complex operation process, and a significant amount of residual raw impurities have limited modified zeolite application in  $\text{NH}_4^+$  adsorption. NaCl-modified zeolite is a common and cheap method and the adsorbent was easily obtained. NaCl

\*Corresponding author, email: [huangxman@vip.sina.com](mailto:huangxman@vip.sina.com)

Received 16 September 2018; accepted in revised form 27 September 2019

modification effectively increased ammonium adsorption capacity by increasing the Na contents in zeolite and by modifying the surface morphology to enhance film mass transfer rate (Lin et al., 2013).

Although a large number of studies related to the removal of ammonium by using types of zeolites have been reported in the literature, zeolites from different locations with special physical and chemical properties require individual investigation (Alshameri et al., 2014; Huang et al., 2010; Malekian et al., 2011; Sarioglu, 2005). The mineral reserve of clinoptilolite in Xuancheng is abundant, and clinoptilolite has significant performance in adsorption of ammonium from aqueous solution. Zeolite modified by sodium chloride solution can have a greatly increased adsorption capacity for ammonium. Therefore, it is important to study the property of ammonium adsorption for natural zeolite (N-Zeo) and NaCl-modified zeolite (M-Zeo). The objectives of this study were: (i) to prepare M-Zeo and systematically investigate its application for  $\text{NH}_4^+$  removal from aqueous solution; (ii) to elucidate the effects of environmental conditions, including pH, initial concentration of ammonium and temperature on the adsorption of ammonium to M-Zeo by batch experiments; (iii) to reveal the exchange selectivity of  $\text{Na}^+$ ,  $\text{Ca}^{2+}$ ,  $\text{K}^+$ ,  $\text{Mg}^{2+}$  contained in zeolite for ammonium; (iv) to study the adsorptive mechanism of  $\text{NH}_4^+$  on M-Zeo through adsorption isotherms, thermodynamic and kinetic models; (v) to discuss the rate-controlled process of  $\text{NH}_4^+$  adsorption onto M-Zeo according to the apparent activation energy; (vi) to investigate the treatment of real wastewater containing ammonium by M-Zeo. The aim of this paper is to evaluate the suitability of M-Zeo as an efficient and low-cost clay adsorbent for adsorption of ammonium from aqueous solution and wastewater in environmental clean-up, and the Arrhenius formula was employed to reveal the rate-controlled process of ammonium adsorption onto M-Zeo.

## MATERIALS AND METHODS

### Materials

Natural zeolite (N-Zeo) used in the experiments was obtained from Xuancheng in Anhui Province, China, which was ground and selected for particle sizes of 45–74 µm. Due to adsorbents with smaller particle size and larger specific surface area showing higher adsorption performance, zeolite powder in the particle size of 45–74 µm was used in this study. Zeolite samples (25 g) were dispersed in 500 mL of 2 mol/L NaCl solution by magnetic stirring for 24 h; the concentration of NaCl used followed Lin et al. (2013). Then the mixtures were centrifuged, washed 5 times with deionized water, and dried at 105°C for 12 h. The obtained NaCl-modified zeolite (M-Zeo) was finally ground and screened though a 200 mesh sieve (74 µm).

Stock ammonium solution (10000 mg  $\text{NH}_4^+$ -N/L) was prepared by dissolving 38.207 g  $\text{NH}_4\text{Cl}$  into 1 L deionized water. All working solutions were prepared by diluting this stock solution with deionized water.

### Batch adsorption experiments

To investigate the impact of pH values on the adsorption capacity of ammonium, natural and modified zeolite were tested. Ammonium solutions (25 mL, 1000 mg/L) were added into 150 mL conical flasks with stoppers, and the pH of

solutions was adjusted to 5, 6, 7, 8, and 9 by adding 0.1–1 M NaOH solution and 0.1–1 M HCl solution. After adding 0.5 g of adsorbent, the flasks were stirred at 200 r/min in thermostatic shakers for 24 h at 293 K. After the mixture was centrifuged, the supernatant was filtered through a 0.45 µm membrane filter prior to the determination of ammonium concentrations. The equilibrium adsorptive capacity was calculated by Eq. 1:

$$q_t = \frac{(C_0 - C_t)V}{W} \quad (1)$$

where  $q_t$  is the adsorptive capacity at time  $t$ , mg/g;  $C_0$  is the initial concentration of ammonium in the solution, mg/L;  $C_t$  is the concentration of ammonium in the solution at time  $t$ , mg/L;  $V$  is the volume of the solution, L; and  $W$  is the mass of the adsorbent, g.

Adsorption isotherms for ammonium were carried out in thermostatic shakers for 24 h at desired temperatures (293, 303, 313 K). Adsorbents (0.5 g) were mixed with ammonium solutions (25 mL) at different initial concentrations ranging from 5 to 1 000 mg/L (5, 10, 25, 50, 100, 200, 500, 800, 1 000 mg/L) at pH 8. The order of exchange selectivity was evaluated by examining the concentrations of cations.

Adsorption kinetics for ammonium were evaluated at pH 8 and at an ambient temperature of 293 K. Adsorbents (0.5 g) were added to ammonium solutions (25 mL) with an initial concentration of 1 000 mg/L. Samples withdrawn at different time intervals of 0.25, 0.5, 1, 2, 3, 4, 8 and 12 h were analysed for ammonium concentration.

The regeneration study was performed by evaluating the effect of regeneration cycles on the ammonium adsorptive capacity at pH 8 and at an ambient temperature of 293 K. Adsorbents (0.5 g) were added in 25 mL of 1 000 mg/L ammonium solutions. The adsorbents were collected after adsorption and regenerated by 250 mL of 2 mol/L NaCl solution; the concentration of NaCl was consistent with the concentration used in the adsorbent preparation. Then, the zeolites were washed by deionized water and centrifuged several times. The regenerated zeolite was reused for adsorption of ammonium from aqueous solution.

### Analysis methods

Ammonium concentrations in liquid samples were analysed by spectrophotometry with a spectrophotometer (V-1100D, Mapada Co., Shanghai, China). The concentrations of  $\text{Na}^+$ ,  $\text{K}^+$ ,  $\text{Ca}^{2+}$  and  $\text{Mg}^{2+}$  in solution were measured by atomic absorption spectroscopy (AAS-6300C, Shimadzu, Japan). Elemental compositions of M-Zeo were determined using X-ray fluorescence (XRF) (XRF-1800, Shimadzu, Japan). Mineral phases were identified by X-ray diffraction (XRD) using a D/max-RB powder diffraction meter (Rigaku, Japan), with a Cu-target operated at 40 kV, 100 mA. The XRD patterns were taken in the range of 4–70° at a scan rate of 4°/min, which were analysed using the software (Search-Match) by comparing the experimental data with those included in the Joint Committee of Powder Diffraction Standards (JCPDSs) database.

## RESULTS AND DISCUSSION

### Characterization

XRD patterns of N-Zeo and M-Zeo are illustrated in Fig. 1. Diffraction patterns at  $2\theta = 9.88, 11.22, 17.34, 22.74, 26.12,$

29.06, and 32° are identified as clinoptilolite when compared with the standard database. The characteristic peaks of quartz can be found at 26.7 and 50.1°. The intensity of quartz became weaker after modification. The XRD spectra of M-Zeo showed no significant differences from N-Zeo, indicating that the main mineral phases of zeolite were not changed after modification.

XRF was applied to analyse the elemental compositions of N-Zeo and M-Zeo, presented as percentage of element in the highest oxidation state (Table 1). It can be clearly seen that the contents of the exchangeable cations such as K<sup>+</sup>, Ca<sup>2+</sup>, and Mg<sup>2+</sup> in the M-Zeo were decreased, while the amount of Na<sup>+</sup> was increased significantly. The result suggested that Ca<sup>2+</sup>, K<sup>+</sup>, and Mg<sup>2+</sup> were replaced by Na<sup>+</sup>, which can be used to remove NH<sub>4</sub><sup>+</sup> in ion-exchange applications.

### Effect of pH

Figure 2a shows the adsorption of ammonium onto N-Zeo and M-Zeo as a function of initial pH. In acidic condition, increasing pH favoured both N-Zeo and M-Zeo adsorption of ammonium. In basic conditions (pH 8 to 10), reduced adsorption capacity with increasing pH is seen in Fig. 2a, leading to the highest adsorption capacities of 11.39 and 17.77 mg/g on N-Zeo and M-Zeo, respectively, at pH 8. This clearly implies that ammonium adsorption onto both N-Zeo and M-Zeo was pH dependent. The dominant mechanism of ammonium adsorption onto N-Zeo and M-Zeo was assumed to be ion-exchange between cations (Na<sup>+</sup>, K<sup>+</sup>, Ca<sup>2+</sup>, Mg<sup>2+</sup>, et al.) on the adsorbent surface and ammonium in the solution. As shown in Fig. 2b, ammonium existed in the form of NH<sub>4</sub><sup>+</sup> in aqueous solution at pH 2–8, and as NH<sub>3</sub> at pH 10–13. The species of ammonium were converted from NH<sub>4</sub><sup>+</sup> to NH<sub>3</sub> when pH was between 8 and 10. At pH < 8, ammonium adsorption increased with increasing pH, principally being attributed to the decline in competing hydrogen ions, and with cation exchange being the dominant

mechanism (Liu et al., 2013). At pH > 8, ammonium removal decreased with increasing pH, likely owing to the conversion of NH<sub>4</sub><sup>+</sup> into NH<sub>3</sub> in alkaline solution. Thus, molecule adsorption was the main mechanism for ammonium removal, which resulted in the reduction of ion-exchange potential. This observation correlated with findings reported in the literature (He et al., 2016; Lin et al., 2013). Therefore, the optimum pH of M-Zeo for adsorption of ammonium is that of a neutral solution.

### Ion-exchange adsorption

The ion exchange process between the zeolite frame and aqueous ammonium solution can be expressed by Eq. 2 (Lin et al., 2013):



where *M* represents the loosely held cations in zeolite and *n* is the number of electric charges. Assuming *M* in zeolite are Na<sup>+</sup>, K<sup>+</sup>, Ca<sup>2+</sup> and Mg<sup>2+</sup>, the ion exchange capacity (IEC) can be calculated as the sum of exchange cations as follows:

$$IEC = [\text{Na}^+] + [\text{K}^+] + 2[\text{Ca}^{2+}] + 2[\text{Mg}^{2+}] = [\text{NH}_4^+] \quad (3)$$

As shown in Fig. 3, the adsorption capacity of ammonium onto M-Zeo increased significantly at different initial ammonium ion concentrations, while the equivalent concentrations of Mg<sup>2+</sup>, K<sup>+</sup>, Na<sup>+</sup> and Ca<sup>2+</sup> released into the solution increased significantly. The IEC for the sum of the four cations was a little lower than the ammonium adsorption capacity at equilibrium, indicating that ion exchange is predominant in the adsorption of ammonium by zeolite. The extra amount of ammonium adsorption on M-Zeo is ascribed to electrostatic attraction between negative charges on the adsorbent surface and NH<sub>4</sub><sup>+</sup> (Alshameri, Ibrahim, et al., 2014).

When the initial ammonium concentration rose to 25 mg/L, K<sup>+</sup> started to be released from zeolite. Mg<sup>2+</sup>

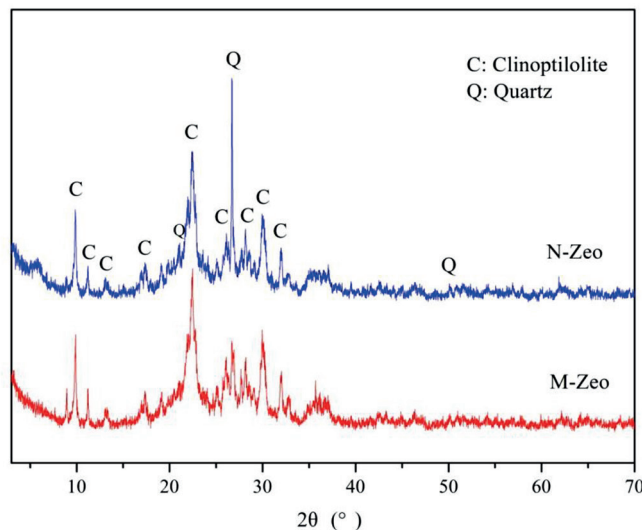


Figure 1. XRD patterns of natural and modified zeolites

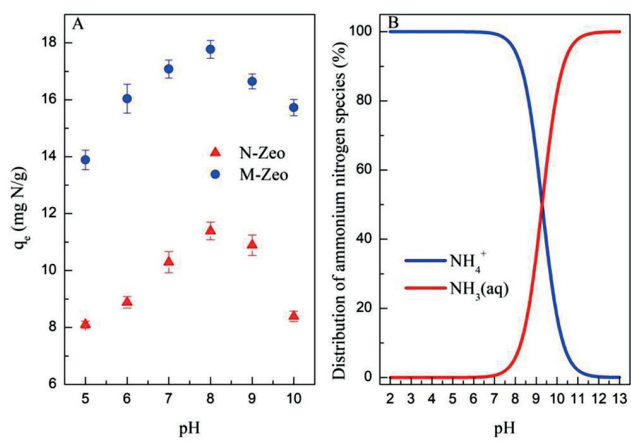
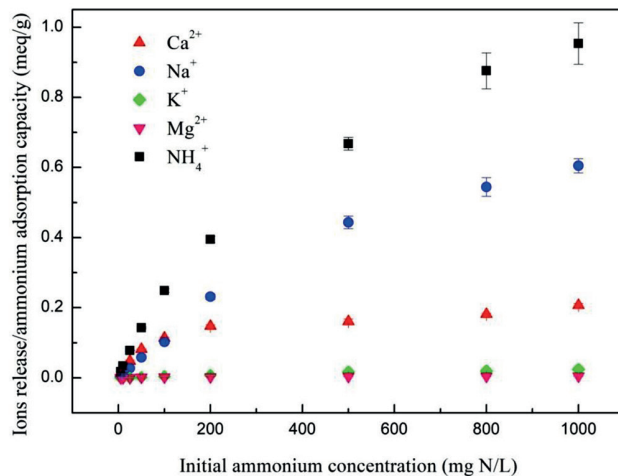


Figure 2. (a) Effect of initial pH on ammonium adsorption on N-Zeo and M-Zeo ( $C_o = 1\,000\text{ mg/L}$ ,  $t = 24\text{ h}$ ,  $T = 293\text{ K}$ ); (b) Distribution of ammonium species in aqueous solutions

Table 1. Chemical composition of natural and modified zeolites (wt.%)

Components	SiO <sub>2</sub>	Al <sub>2</sub> O <sub>3</sub>	CaO	K <sub>2</sub> O	Fe <sub>2</sub> O <sub>3</sub>	MgO	Na <sub>2</sub> O	LOI <sup>a</sup>
N-Zeo	71.36	10.16	2.52	2.48	1.23	1.19	0.41	10.32
M-Zeo	69.54	10.38	2.16	1.17	1.15	0.82	3.89	9.85

<sup>a</sup>Loss on ignition at 1 000°C



**Figure 3.** Ion release and ammonium adsorption capacity of M-Zeo under different initial ammonium concentration conditions ( $C_0 = 5\text{--}1000 \text{ mg/L}$ ,  $\text{pH} = 8$ ,  $t = 24 \text{ h}$ ,  $T = 293 \text{ K}$ )

appeared in the aqueous solution after the initial ammonium concentration rose to 50 mg/L.  $\text{Na}^+$  was the dominant cation exchanged with ammonia under an initial ammonia concentration of less than 100 mg/L, while  $\text{Ca}^{2+}$  was the dominant cation exchanged with ammonia under an initial ammonia concentration higher than 100 mg/L. Thus, the effect of the metal ions on ammonium adsorption to zeolite suggests an order of preference of  $\text{Na}^+ > \text{Ca}^{2+} > \text{K}^+ > \text{Mg}^{2+}$ . A similar result was reported by other researchers (Lin et al., 2013). A slight difference in the order was determined as  $\text{Na}^+ > \text{K}^+ > \text{Ca}^{2+} > \text{Mg}^{2+}$  by other researchers (Lei et al., 2008; Watanabe et al., 2007).

#### Adsorption isotherms

The adsorption isotherms of ammonium on zeolite were fitted by two typical models, Langmuir and Freundlich, as Eqs 4 and 5 (Liu et al., 2013; Langmuir, 1918):

$$\frac{C_e}{q_e} = \frac{1}{q_m} C_e + \frac{1}{q_m k} \quad (4)$$

$$\ln q_e = \ln K_f + \frac{1}{n} \ln C_e \quad (5)$$

where  $C_e$  is the equilibrium concentration (mg/L) in the solution;  $q_e$  is the adsorption capacity on adsorbent (mg/g);  $q_m$  refers to the maximum adsorption capacity at monolayer coverage (mg/g). The values of  $k$  (L/mg) and  $K_f$  (mg/g) are the Langmuir and Freundlich adsorption constants, respectively.  $1/n$  is a constant relating to adsorption intensity or surface heterogeneity.

**Table 2** Relative parameters of the Langmuir, Freundlich and D-R models

Adsorbent	T(K)	Langmuir			Freundlich			D-R			
		$q_m$ (mg/g)	$k$	$R^2$	$K_f$ (mg/g)	$1/n$	$R^2$	$B$ (mol²/J²)	$q_m$ (mg/g)	$E$ (kJ/mol)	$R^2$
N-Zeo	293	13.66	0.016	0.9682	0.66	0.466	0.9991	$5.4 \times 10^{-9}$	13.92	9.62	0.9775
	303	13.97	0.018	0.9770	0.70	0.465	0.9980	$5 \times 10^{-9}$	14.54	10	0.9776
	313	14.27	0.019	0.9802	0.70	0.473	0.9965	$4.8 \times 10^{-9}$	15.64	10.21	0.9851
M-Zeo	293	17.83	0.018	0.9745	0.71	0.511	0.9962	$5.4 \times 10^{-9}$	24.1	9.62	0.9905
	303	18.38	0.022	0.9815	0.83	0.500	0.9933	$4.9 \times 10^{-9}$	25.68	10.1	0.9934
	313	19.98	0.027	0.9883	0.93	0.497	0.9905	$4.5 \times 10^{-9}$	27.54	10.54	0.9933

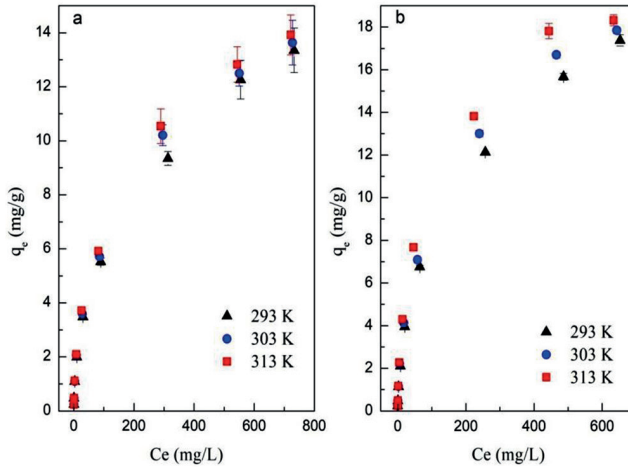


**Figure 4.** The isotherm plots of ammonium adsorption on N-Zeo (a) and M-Zeo (b) ( $C_0 = 5\text{--}1000 \text{ mg/L}$ ,  $\text{pH} = 8$ ,  $t = 24 \text{ h}$ )

The relative parameters ( $q_m$ ,  $k$ ,  $K_f$  and  $1/n$ ) were calculated from the slope and intercept of the linear plots based on the Langmuir and Freundlich adsorption isotherms. As the correlation coefficient of the Freundlich model ( $R^2 > 0.9905$ ) was higher than that of the Langmuir model ( $R^2 < 0.9815$ ), the Freundlich model was suggested to better fit ammonium sorption onto both N-Zeo and M-Zeo. This indicated that adsorption occurred on a structurally heterogeneous adsorbent (Pan et al., 2017). The maximum adsorption capacity on a monomolecular layer of M-Zeo was estimated to be 17.83 mg/g at 293 K, which is higher than that found by other researchers. For example, Mazloomi and Jalali (2016) found the maximum adsorption of ammonium by Iranian zeolite to be 10.08 mg/g. Saltali et al. (2007) reported that the adsorption capacity of ammonium by natural Turkish zeolite was 9.64 mg/g at 294 K (Saltali et al., 2007). It has also been reported that the maximum adsorption of ammonium using a salt-activated Chinese (Hulaodu) zeolite was 9.52 mg/g (Alshameri et al., 2014). Meanwhile the ammonium exchange capacity for natural and modified Yemeni zeolites were 11.18 mg/g and 8.29 mg/g, respectively (Alshameri et al., 2014). The constant of  $1/n$  for the Freundlich model is related to the adsorption intensity, which varies with the heterogeneity of materials. The values of  $1/n$  were lower than 0.52 in this study, which suggests that the adsorption of ammonium on N-Zeo and M-Zeo was highly favourable (Table 2).

The Dubinin-Redushkevich (D-R) isotherm was also employed to reveal the type of adsorption (physical adsorption or chemical adsorption) (Mazloomi and Jalali, 2016). The D-R equation has the linear form:

$$\ln q_e = \ln q_m - \beta \varepsilon^2 \quad (6)$$

where  $q_m$  is the D-R adsorption capacity (mol/g);  $\beta$  is the constant of the adsorption energy (mol<sup>2</sup>/J<sup>2</sup>), related to the average energy of adsorption per mole of the sorbate as it is transferred to the surface of the solid from infinite distance in the solution;  $\varepsilon$  is Polanyi potential, which is described as:

$$\varepsilon = RT \ln\left(1 + \frac{1}{C_e}\right) \quad (7)$$

where  $T$  is the absolute temperature (K) and  $R$  is the gas constant (8.314 J/mol·K).

Moreover, the mean energy of adsorption  $E$  (kJ/mol) can be calculated from the D-R parameter  $\beta$  using the following formula:

$$E = \frac{1}{\sqrt{2\beta}} \quad (8)$$

As seen in Table 2, the correlation coefficients of the D-R model for ammonium sorption on N-Zeo and M-Zeo were higher than 0.977, suggesting the D-R model was acceptably applied to fit the experimental data in this study. The relative parameters ( $\beta$  and  $q_m$ ) were calculated from the slope and intercept of Eq. 6. The value of mean energy of adsorption  $E$  is in the range of 1–8 kJ/mol and 8–16 kJ/mol for physical and chemical adsorption, respectively. In this study, the  $E$  values of ammonium adsorption on N-Zeo and M-Zeo were in the range of 8–16 kJ/mol, indicating that the adsorption process was essentially chemisorption (Table 2).

### Thermodynamic parameters

The thermodynamic parameters can be calculated from the temperature-dependent adsorption isotherms based on Eqs 9–11:

$$K_d = \frac{q_e}{C_e} \quad (9)$$

$$\Delta G^0 = -RT \ln K_d \quad (10)$$

$$\ln K_d = -\frac{\Delta H^0}{RT} + \frac{\Delta S^0}{R} \quad (11)$$

where  $K_d$  is the distribution coefficient, mL/g;  $\Delta G^0$  is the change of Gibbs energy, kJ/mol. The values of enthalpy ( $\Delta H^0$ ) and entropy ( $\Delta S^0$ ) can be obtained by the slope and intercept of the plot of  $\ln K_d$  versus  $1/T$  (Fig. 5). The values of  $K_d$ ,  $\Delta G^0$ ,  $\Delta H^0$  and  $\Delta S^0$  are summarized in Table 3. Negative values of  $\Delta G^0$  and positive values of  $\Delta H^0$  were found, which reveals that the processes of ammonium adsorption on N-Zeo and M-Zeo were endothermic, feasible and spontaneous. The change of entropy ( $\Delta S^0$ ) was 0.032 and 0.038 kJ/(mol·K) for the adsorption of ammonium on N-Zeo and M-Zeo, respectively. The positive values of  $\Delta S^0$  suggested that the randomness increased during the removal of ammonium ions from aqueous solution onto N-Zeo and M-Zeo.

### Adsorption kinetics

The adsorption kinetics of ammonium on M-Zeo and N-Zeo was simulated by four typical kinetic models. The kinetic

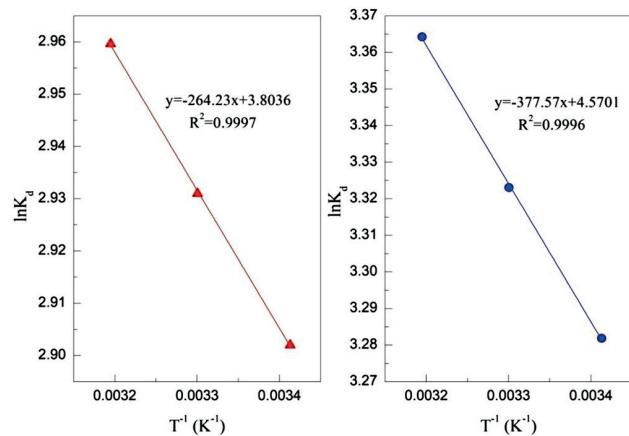


**Figure 5.** Plots of  $\ln K_d$  vs.  $1/T$  (a: N-Zeo; b: M-Zeo)

equations, including pseudo first-order model, pseudo second-order model, Elovich model and intraparticle diffusion model, are described as follows (Huang et al., 2015; Malekian et al., 2011; Yang et al., 2015):

$$\text{Pseudo first-order equation: } \ln(q_e - q_t) = \ln q_e - k_1 t \quad (12)$$

$$\text{Pseudo second-order equation: } \frac{t}{q_t} = \frac{1}{k_2 q_e^2} + \frac{t}{q_e} \quad (13)$$

$$\text{Elovich equation: } q_t = \frac{\ln a_e b_e}{b_e} + \frac{1}{b_e} \ln t \quad (14)$$

$$\text{Intraparticle diffusion equation: } q_t = k_3 t^{0.5} \quad (15)$$

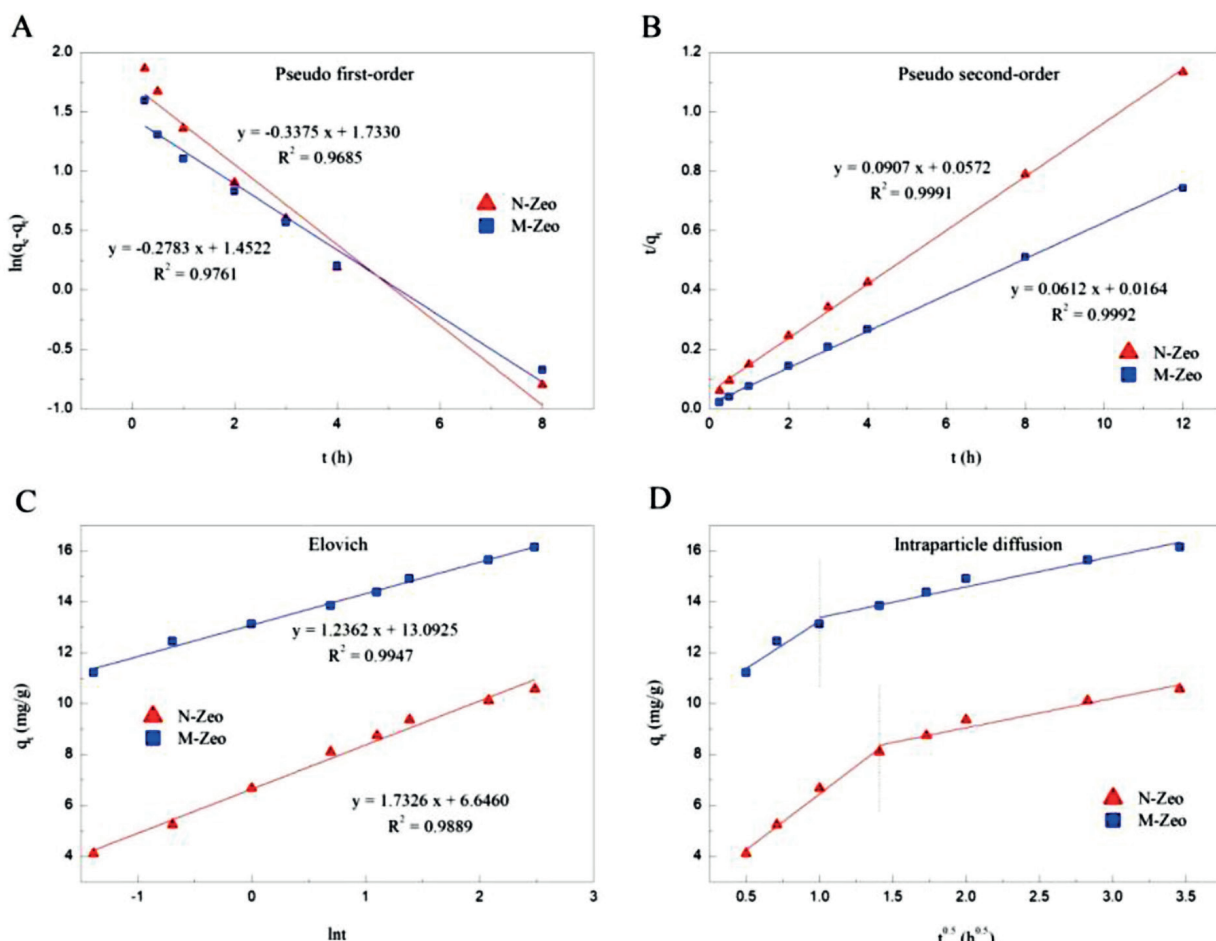
where  $q_t$  is the adsorbed amount at time  $t$ , mg/g;  $q_e$  is the adsorption amount at equilibrium, mg/g;  $k_1$  is the rate constant of pseudo first-order adsorption, g/(mg·h);  $k_2$  is the rate constant of pseudo second-order adsorption, g/(mg·h); the parameter  $a_e$  is the initial adsorption rate, mg/(g·h), and  $b_e$  is related to extent of surface coverage and activation energy for chemisorption, g/mg;  $k_3$  is the intraparticle diffusion rate constant, mg/(g·h<sup>0.5</sup>).

Table 2 tabulates the relative parameters calculated from these four kinetic models. Constants  $k_1$  and  $k_2$  were respectively determined from the slope of the line obtained by plotting  $\ln(q_e - q_t)$  versus  $t$  in the pseudo-first-order model and the intercept of the line by plotting  $t/q_t$  versus  $t$  in the pseudo-second-order model, while the initial adsorption rate  $a_e$  was determined from the intercept of the line obtained by plotting  $q_t$  versus  $\ln t$  in the Elovich equation. The intraparticle diffusion rate constant  $k_3$  was calculated from the slope of the line obtained by plotting  $q_t$  and  $t^{0.5}$ . The correlation coefficient for the pseudo-second-order model is the highest among the four kinetic models, revealing that the pseudo-second-order model best describes the adsorption kinetics of ammonium onto M-Zeo, and that chemisorption dominates in the adsorption process (Huang et al., 2017; Liao et al., 2012). This conclusion matched the fitting results from the D-R isotherm. Moreover, the theoretically adsorbed amount at equilibrium (16.34 mg/g) obtained from the pseudo-second-order model was much closer to the adsorbed amount at equilibrium obtained from experiment (17.83 mg/g) than that obtained from the other models. Due to the high correlation coefficient (>0.99), the Elovich equation was also found to be suitable to describe the second-order kinetic, assuming that the actual solid surfaces

are energetically heterogeneous (Mezenner and Bensmaili, 2009). The initial adsorption rate  $a_e$  was 49.166 mg/(g·h) for ammonium adsorption onto M-Zeo, which was much higher than 80.27 mg/(g·h) for ammonium adsorption onto N-Zeo. The intraparticle diffusion model is assumed to be the sole rate-controlling step if the regression of  $q_t$  versus  $t^{0.5}$  is linear and the plots pass through the origin (Huang et al., 2010). The fitting results show that the regression was linear, but the plot did not pass through the origin. As seen in Fig. 6d, the ammonium adsorption onto N-Zeo and M-Zeo involved two steps and presented a multilinearity. Therefore, the adsorption processes of ammonium onto N-Zeo and M-Zeo can be divided into two steps. The first, fast step was mainly contributed by boundary layer diffusion or macro-pore diffusion. The second, gradual step was attributed to intraparticle diffusion or micro-pore diffusion (Pan et al., 2017; Widiastuti et al., 2011).

**Table 3.** Thermodynamic parameters of ammonium adsorption onto N-Zeo and M-Zeo

Adsorbent	T (K)	$q_e$ (mg/g)	$C_e$ (mg/g)	$K_d$ (mL/g)	$\Delta G^\circ$ (kJ/mol)	$\Delta H^\circ$ (kJ/mol)	$\Delta S^\circ$ (kJ/mol·K)
N-Zeo	293	13.35	733.02	18.21	-7.069	2.197	0.032
	303	13.63	727.32	18.75	-7.384		
	313	13.92	721.59	19.29	-7.702		
M-Zeo	293	17.37	652.52	26.63	-7.995	3.139	0.038
	303	17.84	643.13	27.74	-8.371		
	313	18.32	633.62	28.91	-8.755		



**Figure 6.** Kinetic models of adsorption of ammonium on N-Zeo and M-Zeo: a: the pseudo-first-order model, b: the pseudo-second-order model, c: the Elovich model, d: the intraparticle diffusion model ( $C_0 = 1\,000$  mg/L, pH = 8,  $t = 24$  h,  $T = 293$  K)

## The apparent activation energy

The linear form of the Arrhenius equation can be expressed as the following formula:

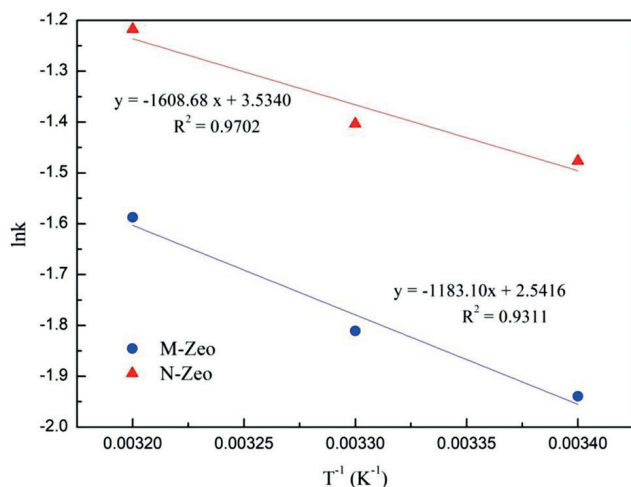
$$\ln k = -\frac{E_a}{RT} + \ln A \quad (16)$$

where  $k$  is the rate constant of pseudo second-order adsorption;  $E_a$  is the apparent activation energy, J/mol;  $R$  is the gas constant, 8.314 J/mol·K;  $T$  is the absolute temperature (K).

Comparison of the outputs of adsorption kinetics models suggested that the adsorption process of ammonium onto N-Zeo and M-Zeo was in accordance with the pseudo-second order model. Thus, the apparent activation energy can be determined by the slope of the line plotting  $\ln k$  ( $k_2$  in Table 4) versus  $1/T$  according to the Arrhenius equation. Chen (2016) stated that the reaction rate would be fast if  $E_a$  is less than

**Table 4.** Kinetic parameters of ammonium adsorption onto N-Zeo and M-Zeo

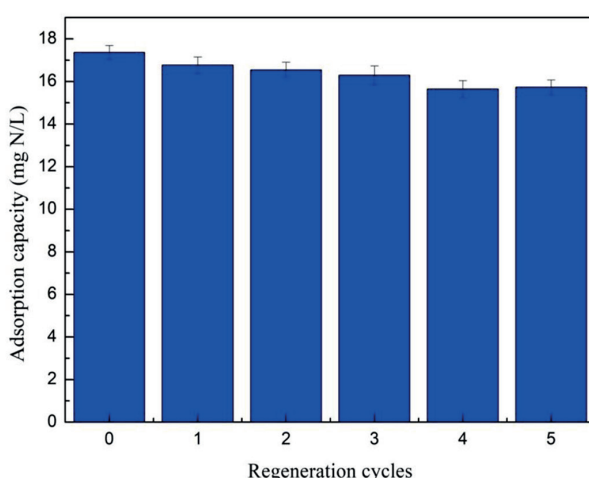
Kinetic model	Pseudo first-order			Pseudo second-order			Simple Elovich			Intraparticle diffusion	
	$q_e$ (mg/g)	$k_1$ (h <sup>-1</sup> )	$R^2$	$q_e$ (mg/g)	$k_2$ (g/[mg·h])	$R^2$	$a_e$ (mg/[g·h])	$b_e$ (g/mg)	$R^2$	$k_3$ (mg/[g·h <sup>0.5</sup> ])	$R^2$
N-Zeo	5.66	0.3375	0.9685	11.12	0.1438	0.9991	80.27	0.577	0.9889	2.0989	0.8676
M-Zeo	4.27	0.2783	0.9761	16.34	0.2284	0.9992	49166	0.809	0.9947	1.5334	0.9150

**Figure 7.** The linear fitting of Arrhenius equation

40 kJ/mol at room temperature, and rather slow if  $E_a$  is greater than 120 kJ/mol (Chen et al., 2016). Moreover, adsorption would be a diffusion-controlled process if the  $E_a$  is less than 25–30 kJ/mol (Lazaridis and Asouhidou, 2003; Mezennier and Bensmaili, 2009). In the present study,  $E_a$  was 13.37 kJ/mol for ammonium adsorption onto N-Zeo and 9.84 kJ/mol for ammonium adsorption onto M-Zeo, which was less than 25 kJ/mol. Thus, the adsorption of ammonium on M-Zeo was a fast and diffusion-controlled process and its reaction rate was much higher than the adsorption of ammonium on N-Zeo.

#### Regeneration and treatment of real wastewater

Fig. 8 shows the regeneration of M-Zeo after adsorbing ammonium. After being regenerated after the first cycle, the adsorption capacity of ammonium onto M-Zeo was slightly decreased from 17.36 mg/g to 16.77 mg/g. After 5 cycles in regeneration, the adsorption capacity had dropped to 15.73 mg/g and the regeneration ratio was up to 90.61%. A similar result was reported by Ji et al. (2007). Treatment of real wastewater by adsorbents could evaluate if the adsorbents can be used for environmental purification (Kostic et al., 2017; Kostic et al., 2018). In this study, sewage, which was collected from a domestic wastewater pipe at Xiamen University of Technology campus, with an initial ammonium concentration of 14.92 mg/L was employed to estimate the possibility of M-Zeo being used for real wastewater treatment. Under the condition of a pH value of 8.5 for the campus sewage, the final concentration of ammonium was 0.13 mg/L, indicating a removal efficiency for ammonium of 99.13%. Given the high removal efficiency and regeneration ratio of M-Zeo, it can be considered as a promising adsorbent in the preconcentration and removal of ammonium from aqueous solutions in environmental clean-ups.

**Figure 8.** Adsorption capacities after each of 5 regeneration cycles ( $C_0 = 1\,000$  mg/L, pH = 8,  $t = 24$  h,  $T = 293$  K)

#### CONCLUSIONS

The synthetic M-Zeo was successfully prepared from N-Zeo by dispersing into NaCl solution and drying at 105°C. The adsorption isotherms and kinetics of ammonium by M-Zeo could be satisfactorily simulated by the Freundlich model and the pseudo-second-order model, respectively. Thermodynamic parameters indicated that the adsorption process of ammonium onto M-Zeo was endothermic and spontaneous. The fitting results of the D-R isotherm determined that ammonium removal by M-Zeo was chemisorption. According to the intraparticle diffusion model, ammonium adsorption onto M-Zeo involved two adsorption steps: (i) boundary layer diffusion or macro-pore diffusion, and (ii) intraparticle diffusion or micro-pore diffusion. The  $E_a$  in the Arrhenius equation suggested that the adsorption of ammonium on M-Zeo was a fast and diffusion-controlled process. The findings of this study suggest that the low cost, high adsorption capacity and good regeneration performance of M-Zeo indicate that it is a promising adsorbent to be widely utilized for ammonium removal from aqueous solution.

#### ACKNOWLEDGEMENTS

The authors would like to express their gratitude for the financial support provided by the Natural Science Foundation of Fujian Province, China (2016J05140), the Open Research Fund Program from Key Laboratory of Environmental Biotechnology (XMUT), Fujian Province University (EBL2018004), the Scientific Research Project of Xiamen Overseas Talents (201631402), Scientific Climbing Program of Xiamen University of Technology (XPDKQ18031) and the Science and Technology Project of Longyan City (2017LY63).

## REFERENCES

- ALSHAMERI A, IBRAHIM A, ASSABRI AM, LEI X, WANG H and YAN C (2014) The investigation into the ammonium removal performance of Yemeni natural zeolite: Modification, ion exchange mechanism, and thermodynamics. *Powder Technol.* **258** 20–31. <https://doi.org/10.1016/j.powtec.2014.02.063>
- ALSHAMERI A, YAN C, AL-ANI Y, DAWOOD AS, IBRAHIM A, ZHOU C and WANG H (2014) An investigation into the adsorption removal of ammonium by salt activated Chinese (Hulaodu) natural zeolite: Kinetics, isotherms, and thermodynamics. *J. Taiwan Inst. Chem. Eng.* **45** 554–564. <https://doi.org/10.1016/j.jtice.2013.05.00>
- CHEN F, ZHOU C, LI G and PENG F (2016) Thermodynamics and kinetics of glyphosate adsorption on resin D301. *Arab. J. Chem.* **9** S1665–S1669. <https://doi.org/10.1016/j.arabjc.2012.04.014>
- DARAMOLA M, ARANSIOLA E and OJUMU T (2012) Potential applications of zeolite membranes in reaction coupling separation processes. *Materials* **5** 2101–2136. <https://doi.org/10.3390/ma5112101>
- HE Y, LIN H, DONG Y, LIU Q and WANG L (2016) Simultaneous removal of ammonium and phosphate by alkaline-activated and lanthanum-impregnated zeolite. *Chemosphere* **164** 387–395. <https://doi.org/10.1016/j.chemosphere.2016.08.110>
- HUANG H, XIAO X, YAN B and YANG L (2010) Ammonium removal from aqueous solutions by using natural Chinese (Chende) zeolite as adsorbent. *J. Hazardous Mater.* **175** 247–252. <https://doi.org/10.1016/j.jhazmat.2009.09.156>
- HUANG H, YANG L, XUE Q, LIU J, HOU L and DING L (2015) Removal of ammonium from swine wastewater by zeolite combined with chlorination for regeneration. *J. Environ. Manage.* **160** 333–341. <https://doi.org/10.1016/j.jenvman.2015.06.039>
- HUANG X, CHEN T, ZOU X, ZHUM, CHEN D and PAN M (2017) The Adsorption of Cd(II) on Manganese oxide investigated by batch and modeling techniques. *Int. J. Environ. Res. Public Health* **14** 1145–1155. <https://doi.org/10.3390/ijerph14101145>
- HUSSAIN S, AZIZ HA, ISA MH, ADLAN MN and ASAARI FA (2007) Physico-chemical method for ammonia removal from synthetic wastewater using limestone and GAC in batch and column studies. *Bioresour. Technol.* **98** 874–880. <https://doi.org/10.1016/j.biortech.2006.03.003>
- JI ZY, YUAN JS and LI XG (2007) Removal of ammonium from wastewater using calcium form clinoptilolite. *J. Hazardous Mater.* **141** 483–488. <https://doi.org/10.1016/j.jhazmat.2006.07.010>
- KARAPINAR N (2009) Application of natural zeolite for phosphorus and ammonium removal from aqueous solutions. *J. Hazardous Mater.* **170** 1186–1191. <https://doi.org/10.1016/j.jhazmat.2009.05.094>
- KOLAKOVIC S, STEFANOVIĆ D, LEMIC J, MILICEVIC D, TOMOVIC S, TRAJKOVIC S and MILENKOVIĆ S (2014) Forming a filter media from zeolite modified with SDBAC for wastewater treatment process. *Chem. Ind. Chem. Eng. Q.* **20** 361–369. <https://doi.org/10.2298/ciceq121218018k>
- KOSTIC M, DORDEVIC M, MITROVIC J, VELINOV N, BOJIC D, ANTONIJEVIC M and BOJIC A (2017) Removal of cationic pollutants from water by xanthated corn cob: optimization, kinetics, thermodynamics, and prediction of purification process. *Environ. Sci. Pollut. Res. Int.* **24** 17790–17804. <https://doi.org/10.1007/s11356-017-9419-1>
- KOSTIC M, RADOVIC M, VELINOV N, NAJDANOVIC S, BOJIC D, HURT A and BOJIC A (2018) Synthesis of mesoporous triple-metal nanosorbent from layered double hydroxide as an efficient new sorbent for removal of dye from water and wastewater. *Ecotoxicol. Environ. Saf.* **159** 332–341. <https://doi.org/10.1016/j.ecoenv.2018.05.015>
- LANGMUIR I (1918) The adsorption of gases on plane surfaces of glass, mica and platinum. *J. Am. Chem. Soc.* **40** 1316–1403. <https://doi.org/10.1021/ja02242a004>
- LAZARIDIS NK and ASOUHIDOU DD (2003) Kinetics of sorptive removal of chromium(VI) from aqueous solutions by calcined Mg-Al-CO<sub>3</sub> hydrotalcite. *Water Res.* **37** 2875–2882. [https://doi.org/10.1016/s0043-1354\(03\)00119-2](https://doi.org/10.1016/s0043-1354(03)00119-2)
- LEI L, LI X and ZHANG X (2008) Ammonium removal from aqueous solutions using microwave-treated natural Chinese zeolite. *Sep. Purif. Technol.* **58** 359–366. <https://doi.org/10.1016/j.seppur.2007.05.008>
- LI M, ZHU X, ZHU F, REN G, CAO G and SONG L (2011) Application of modified zeolite for ammonium removal from drinking water. *Desalination* **271** 295–300. <https://doi.org/10.1016/j.desal.2010.12.047>
- LIAO P, YUAN S, ZHANG W, TONG M and WANG K (2012) Mechanistic aspects of nitrogen-heterocyclic compound adsorption on bamboo charcoal. *J. Colloid Interf. Sci.* **382** 74–81. <https://doi.org/10.1016/j.jcis.2012.05.052>
- LIN L, LEI Z, WANG L, LIU X, ZHANG Y, WAN C, LEE D-J and TAY JH (2013) Adsorption mechanisms of high-levels of ammonium onto natural and NaCl-modified zeolites. *Sep. Purif. Technol.* **103** 15–20. <https://doi.org/10.1016/j.seppur.2012.10.005>
- LIU H, PENG S, SHU L, CHEN T, BAO T and FROST RL (2013) Effect of Fe<sub>3</sub>O<sub>4</sub> addition on removal of ammonium by zeolite NaA. *J. Colloid Interf. Sci.* **390** 204–210. <https://doi.org/10.1016/j.jcis.2012.09.010>
- LIU Z, CHEN L, ZHANG Z, LI Y, DONG Y and SUN Y (2013) Synthesis of multi-walled carbon nanotube–hydroxyapatite composites and its application in the sorption of Co(II) from aqueous solutions. *J. Mol. Liq.* **179** 46–53. <https://doi.org/10.1016/j.molliq.2012.12.011>
- MALEKIAN R, ABEDI-KOUPAI J, ESLAMIAN SS, MOUSAVI SF, ABBASPOUR KC and AFYUNI M (2011) Ion-exchange process for ammonium removal and release using natural Iranian zeolite. *Appl. Clay. Sci.* **51** 323–329. <https://doi.org/10.1016/j.clay.2010.12.020>
- MAZLOOMI F and JALALI M (2016) Ammonium removal from aqueous solutions by natural Iranian zeolite in the presence of organic acids, cations and anions. *J. Environ. Chem. Eng.* **4** 1664–1673. <https://doi.org/10.1016/j.jece.2015.11.031>
- MEZENNER NY and BENSMAILI A (2009) Kinetics and thermodynamic study of phosphate adsorption on iron hydroxide–eggshell waste. *Chem. Eng. J.* **147** 87–96. <https://doi.org/10.1016/j.cej.2008.06.024>
- ONYANGO M, KITTINYA J, HADEBE N, OJIJO V and OCHIENG A (2011) Sorption of melanoidin onto surfactant modified zeolite. *Chem. Ind. Chem. Eng. Q.* **17** 385–395. <https://doi.org/10.2298/ciceq110125025o>
- PAN M, HU Z, LIU R and ZHAN X (2015) Effects of loading rate and aeration on nitrogen removal and N<sub>2</sub>O emissions in intermittently aerated sequencing batch reactors treating slaughterhouse wastewater at 11°C. *Bioprocess Biosyst. Eng.* **38** 681v689. <https://doi.org/10.1007/s00449-014-1307-1>
- PAN M, HUANG X, WU G, HU Y, YANG Y and ZHAN X (2017) performance of denitrifying phosphate removal via nitrite from slaughterhouse wastewater treatment at low temperature. *Water* **9** 818. <https://doi.org/10.3390/w9110818>
- PAN M, LIN X, XIE J and HUANG X (2017) Kinetic, equilibrium and thermodynamic studies for phosphate adsorption on aluminum hydroxide modified palygorskite nano-composites. *RSC Adv.* **7** 4492–4500. <https://doi.org/10.1039/c6ra26802a>
- SALTALI K, SARI A and AYDIN M (2007) Removal of ammonium ion from aqueous solution by natural Turkish (Yildizeli) zeolite for environmental quality. *J. Hazardous Mater.* **141** 258–263. <https://doi.org/10.1016/j.jhazmat.2006.06.124>
- SARIOGLU M (2005) Removal of ammonium from municipal wastewater using natural Turkish (Doganetepe) zeolite. *Sep. Purif. Technol.* **41** 1–11. <https://doi.org/10.1016/j.seppur.2004.03.008>
- WANG Y, LIN F and PANG W (2008) Ion exchange of ammonium in natural and synthesized zeolites. *J. Hazardous Mater.* **160** 371–375. <https://doi.org/10.1016/j.jhazmat.2008.03.006>
- WATANABE Y, YAMADA H, KOKUSEN H, TANAKA J, MORIYOSHI Y and KOMATSU Y (2007) Ion exchange behavior of natural zeolites in distilled water, hydrochloric acid, and ammonium chloride solution. *Sep. Sci. Technol.* **38** 1519–1532. <https://doi.org/10.1081/ss-120019090>
- WIDIASTUTI N, WU H, ANG HM and ZHANG D (2011) Removal of ammonium from greywater using natural zeolite. *Desalination* **277** 15–23. <https://doi.org/10.1016/j.desal.2011.03.030>

<https://doi.org/10.17159/wsa/2019.v45.i4.7546>

Available at <https://www.watersa.net>

ISSN 1816-7950 (Online) = Water SA Vol. 45 No. 4 October 2019

Published under a Creative Commons Attribution 4.0 International Licence (CC BY 4.0)

YANG S, DING C, CHENG W, JIN Z and SUN Y (2015) Effect of microbes on Ni(II) diffusion onto sepiolite. *J. Mol. Liq.* **204** 170–175.  
<https://doi.org/10.1016/j.molliq.2015.01.035>  
ZHAO Y, ZHANG B, ZHANG X, WANG J, LIU J and CHEN R (2010)

Preparation of highly ordered cubic NaA zeolite from halloysite mineral for adsorption of ammonium ions. *J. Hazardous Mater.* **178** 658–664. <https://doi.org/10.1016/j.jhazmat.2010.01.136>